

Optical transmission of periodic annular apertures in metal film on high-refractive index substrate: The role of the nanopillar shape

J.-S. Bouillard,^{1,a)} J. Einsle,¹ W. Dickson,¹ S. G. Rodrigo,² S. Carretero-Palacios,² L. Martin-Moreno,² F. J. Garcia-Vidal,³ and A. V. Zayats¹

¹Centre for Nanostructured Media, IRCEP, The Queen's University of Belfast, Belfast BT7 1NN, United Kingdom

²Departamento de Física de la Materia Condensada and Instituto de Ciencia de Materiales de Aragón, CSIC-Universidad de Zaragoza, E-50009 Zaragoza, Spain

³Departamento de Física Teórica de la Materia Condensada, Universidad Autónoma de Madrid, Madrid 28049, Spain

(Received 10 March 2010; accepted 30 March 2010; published online 17 May 2010)

The influence of annular aperture parameters on the optical transmission through arrays of coaxial apertures in a metal film on high refractive index substrates has been investigated experimentally and numerically. It is shown that the transmission resonances are related to plasmonic crystal effects rather than frequency cutoff behavior associated with annular apertures. The role of deviations from ideal aperture shape occurring during the fabrication process has also been studied. Annular aperture arrays are often considered in many applications for achieving high optical transmission through metal films and understanding of nanofabrication tolerances are important. © 2010 American Institute of Physics. [doi:10.1063/1.3427390]

Annular aperture arrays (AAA), consisting of subwavelength coaxial apertures in metal films,^{1–6} are currently considered an important extension of the plasmonic nanostructures for achieving enhanced transmission of light through opaque materials.^{7,8} There have been studies considering AAA on glass substrates in the near-infrared and visible spectral ranges. Such nanostructures provide additional functionalities compared to simple circular apertures having very high absolute transmission, related to specific waveguided modes in annular apertures, absent in simple circular holes. Coupled to surface plasmon polariton (SPP) modes on metal film interfaces, these modes provide the possibility to achieve high transmission, field enhancement as well as high extraction efficiency of light trapped in the substrate. The latter is especially important for high-refractive index substrates with small angles of total internal reflection. Therefore, such nanostructures may become important in a wide range of applications for light extraction from light-emitting diodes (LEDs), organic LEDs, vertical-cavity surface-emitting lasers (VCSELs), etc.^{9–11} At the same time, studies of the enhanced optical transmission through the plasmonic structures on high-refractive index substrates are virtually absent, despite their potential interest for applications.

In this paper, we present systematic studies of the enhanced transmission through the AAA and its dependence on the size, shape, and period of the plasmonic nanostructures on high refractive index substrates, emulating plasmonic structures on LED chips. The influence of nanofabrication tolerances on the optical properties of plasmonic AAA on high-index substrates is also investigated.

We have studied AAA fabricated in a 100 nm thick Au film on gallium phosphide (GaP) substrate ($n = 3.14–3.59$ in the visible spectral range). Four different types of arrays of annular holes with a constant outer diameter of 200 nm and four different inner diameters: 0 (circular

holes), 50, 75, and 100 nm have been considered. Arrays have been created using a square lattice with three different periods: 600, 650, and 700 nm. The structures were fabricated using a focused ion beam (FIB) milling on magnetron sputtered Au films.

Scanning electron microscopy (SEM) and atomic force microscopy (AFM) were used to characterize the structural integrity and parameters of the arrays. The measurements confirmed good correspondence between the designed and actual parameters of the structures in terms of lateral sizes [Fig. 1(a)]. The profiles of the central pillar were, however, strongly dependent on the FIB milling parameters and for high beam currents, the FIB beam tail is too large to obtain a central nanopillar with a height equal to that of the walls of the aperture. Therefore, in order to obtain the best shape possible, low beam currents were used, typically 10 or 30 pA. The beam tail was also taken into account when creating the pattern file. However, even considering these effects, ideal annular apertures are difficult to obtain on the required length scales [Fig. 1(b)]. Similar deviations and lack of control of the shape on such length scale are common also for other nanofabrication techniques such as nanoimprint and

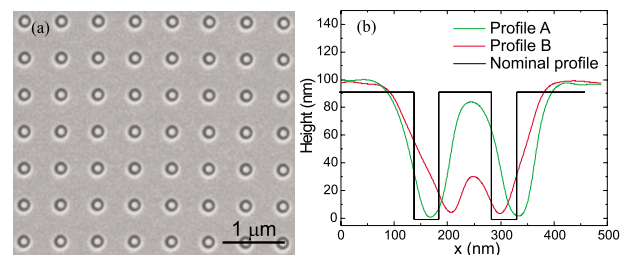


FIG. 1. (Color online) (a) SEM image of a typical array of the FIB-milled annular apertures. (b) The cross-sections of AFM images showing the annular aperture profile for 100 nm inner diameter and 200 nm outer diameter apertures in the 600 nm period array milled with different FIB parameters.

^{a)}Electronic mail: j.bouillard@qub.ac.uk.

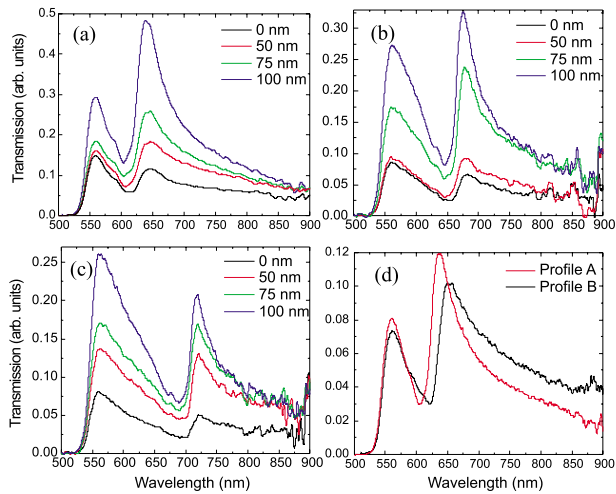


FIG. 2. (Color online) Experimental transmission spectra of the aperture arrays fabricated in the 100 nm thick Au films on the GaP substrate for different periods of the array: (a) 600, (b) 650, and (c) 700 nm. The outer diameter of the apertures is 200 nm, the inner diameters are indicated in the legends. (d) Experimental transmission spectra of the AAA with different profiles of the central nanopillar, corresponding to the AFM images of Fig. 1(b).

femtosecond two-photon nanostructuring that are most suitable for the inexpensive mass-production of such arrays for photonic applications.

Optical characterization was performed by measuring transmission spectra of the arrays at various angles of incidence and light polarizations. Collimated light from a tungsten-halogen lamp was passed through a polarizing cube before illuminating the sample, through the substrate. A long-working-distance objective (50 \times) was used to collect the light transmitted through the structure. Part of the light passed through a beam splitter onto a charge-coupled device (CCD) camera to visualize the illuminated area of the sample surface, with the reflected light passing through an analyzing polarizer cube, with axis oriented parallel to the illumination polarization, before being coupled into an optical fiber. The fiber was used to guide the optical signal to a spectrometer equipped with a liquid nitrogen cooled CCD camera.

For comparison with experimental results, the zeroth order transmission spectrum of each structure has been calculated using the finite-difference time-domain method (FDTD). The calculations were made taking into account a substrate with $n=3.59$ coated with 100 nm of Au. The Au dielectric constant is taken from the experimental data (Ref. 12) implemented in the FDTD formalism as described in Refs. 13 and 14. The dispersion of the refractive index and absorption of GaP substrates were neglected for technical reasons, but the comparison with experiments shows that this is not an important effect for wavelengths longer than 550 nm.

The transmission spectra of the SPP crystals described above are presented in Fig. 2 for different annular apertures and lattice periods. Please note that the strong extinction for wavelengths shorter than 550 nm is due to the strong absorption of GaP substrate in this spectral range.¹⁵ In general, the transmission spectra exhibit one dominating resonance with a period-dependent spectral position. Increasing the diameter of the inner pillar leads to a significant increase in transmission despite the reduction in the total area of the openings. This is accompanied by a small redshift of the

transmission peak position. The maximum transmission was experimentally observed for AAA with inner diameters of approximately 100 nm.

The spectra of the AAA milled with different parameters and therefore featuring differently shaped central nanopillars [Fig. 1(b)] are shown in Fig. 2(d). The two nanopillar types are designated “A” (tall) and “B” (short); they have different heights and while the aperture outer diameter is approximately the same, the effective diameter is different for each nanopillar. While exhibiting a similar spectrum defined by the SPP Bloch mode of the crystal, the resonant transmission of sample B is redshifted and slightly smaller than for the array with taller nanopillars.

Simple analysis of plasmonic modes supported by the nanostructures under consideration shows that SPPs are not supported on the GaP/Au interface in the visible spectral range, since $\epsilon_{\text{Au}} + \epsilon_{\text{GaP}} > 0$ for $\lambda < 620$ nm. Although SPPs exist at lower frequencies, their wavelength is much shorter than that at the Au/air interface and the propagation length is small in the visible spectral range due to the high-refractive index of the GaP. This considerably simplifies the discussion of the transmission mechanisms that, therefore, mainly involve waveguided modes (photonic and/or plasmonic) in annular apertures and SPP Bloch modes on the air/Au interface of the plasmonic crystal.^{16,17} The efficiency with which the waveguided modes transmit energy depends on the thickness of the film as well as the inner and outer diameters of the annular apertures as the propagation constant of the mode depends on these parameters. These waveguided modes are then hybridized with SPP Bloch modes of the crystal lattice which are then coupled to photons. Therefore, the modification of the lattice period leads to the modification of the spectral position of the available SPP Bloch states and their overlap with the waveguided modes. This translates into both a redshift of the transmission peaks and the reduction in the absolute transmittance as the period increases.

Numerical modeling reproduces not only the experimental transmission spectra with good agreement but also the trends observed when the inner diameter and the pillar heights are varied (Figs. 3 and 4). The spectra obtained with the ideal apertures show that the transmission increases in the dominating resonance with an increase in the nanopillar diameter. The position of the peak is strongly sensitive to nanopillar diameter and exhibits a strong redshift when the nanopillar diameter becomes close to the aperture diameter. Since the absorption in the substrate is neglected, the second resonance is observed on the short-wavelength side of the SPP band gap. A good agreement between theory and experiment is observed for the position of each transmission peak as well as the relative transmitted intensity for each structure. Please note that the experiment and modeling are compared for zeroth-order transmission; the calculated total transmission can be up to 20%.

The transmission spectra modeled for different heights of the central pillar are shown in Fig. 4. Again, increasing the nanopillar height leads to an increase in the transmission of the AAA. Initially, the resonance redshifts in comparison to the simple hole resonance until the nanopillar height is half of the film thickness; for taller nanopillars the opposite trend, a blueshift of the resonance, is observed. However, the resonance on the short-wavelength side of the band gap behaves monotonically.

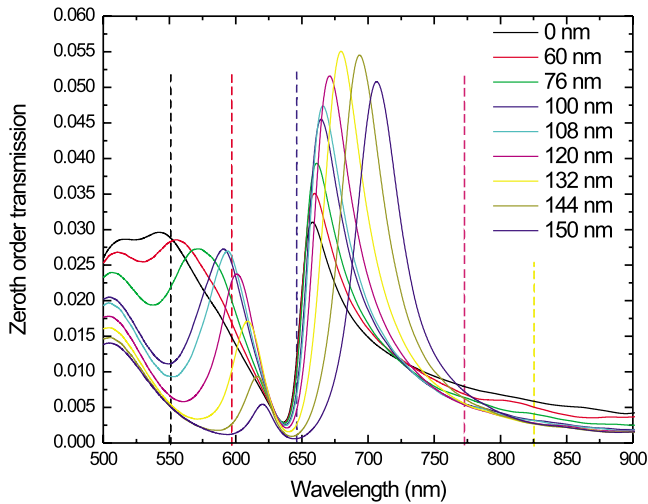


FIG. 3. (Color online) Calculated transmission spectra of the AAA in Au film for different diameters of the inner nanopillar. GaP substrate is considered dispersionless and lossless in the calculations. The film thickness is 100 nm, the period is 650 nm, and the outer diameter of the apertures is 200 nm. The inner diameters are indicated in the legends. The dashed vertical lines indicate the cutoff wavelengths for holes and annular apertures of several inner diameters.

Finally, modeling the transmission spectra using the experimentally acquired profiles almost perfectly recovers the observed experimental spectra (Fig. 4). In these spectra, the short wavelength peak near the absorption edge of the GaP is not resolved, clearly as a result of the nanopillar profile and not the dispersion of the optical properties of the substrate is the reason. In both the experiment and model, it is also clear that this peak is present as a broad shoulder. The interplay

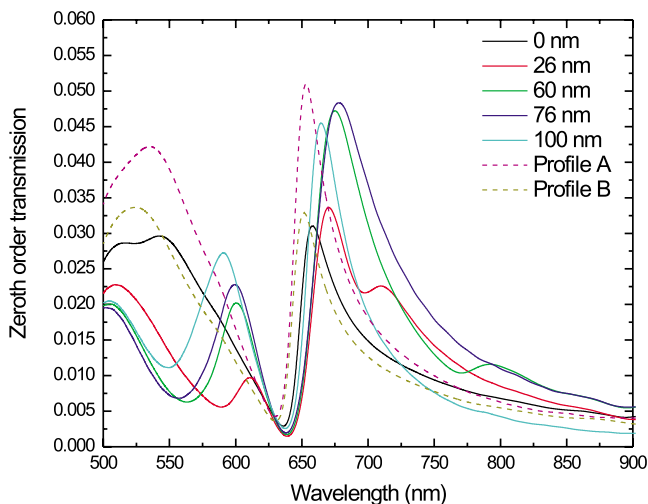


FIG. 4. (Color online) Calculated transmission spectra of the AAA in Au film for different heights of the inner nanopillar. GaP substrate is considered dispersionless and lossless in the calculations. The film thickness is 100 nm, the period is 650 nm, the outer diameter of the apertures is 200 nm, and the inner diameter is 100 nm. The transmission spectra calculated for real nanopillar shapes, as in Fig. 1(b) are also presented.

between variations in both the effective diameter and pillar height, having opposite trends, minimizes the shift of the resonant wavelength but has an impact on the absolute transmission.

In conclusion, we have studied the influence of the nanopillar shape on the resonant transmission through AAA in Au film on a high-refractive index substrate. High-refractive index substrates prevent the efficient use of the SPP modes on Au/substrate interface for tailoring the transmission properties, however by varying the nanostructure parameters some degree of tunability may be achieved. At the same time, simplification of the available SPP Bloch mode spectrum leads to the observed spectral response which is robust over a range of fabrication tolerances, however the absolute transmission is significantly influenced. Such AAA structures may find applications in light extraction and emission conditioning from semiconductor devices such as LEDs and VCSELs.

This work was supported in part by EPSRC (UK) and EC FP6 STREP PLEAS: Plasmon Enhanced Photonics. SGR, SCP, LMM, and FJGV would like to acknowledge support from the Spanish Ministry of Science under Project No. MAT2008-06609-C02. The authors acknowledge fruitful discussions with R. Windisch.

- ¹F. I. Baida and D. Van Labeke, *Phys. Rev. B* **67**, 155314 (2003).
- ²F. I. Baida, D. Van Labeke, G. Granet, and A. Monoreau, *Appl. Phys. B: Lasers Opt.* **79**, 1 (2004).
- ³S. M. Orbons and A. Roberts, *Opt. Express* **14**, 12623 (2006).
- ⁴F. I. Baida, A. Belkhir, and D. Van Labeke, *Phys. Rev. B* **74**, 205419 (2006).
- ⁵M. Haftel, C. Schlockermann, and G. Blumberg, *Phys. Rev. B* **74**, 235405 (2006).
- ⁶J. Salvi, M. Roussey, F. I. Baida, M.-P. Bernal, A. Mussot, T. Sylvestre, H. Maillotte, D. Van Labeke, A. Perentes, I. Utke, C. Sandu, P. Hoffmann, and B. Dwir, *Opt. Lett.* **30**, 1611 (2005).
- ⁷T. W. Ebbesen, H. J. Lezec, H. F. Ghaemi, T. Thio, and P. A. Wolff, *Nature (London)* **391**, 667 (1998).
- ⁸For a recent review see, F. J. Garcia-Vidal, L. Martín-Moreno, T. W. Ebbesen, and L. K. Kuipers, *Rev. Mod. Phys.* **82**, 729 (2010).
- ⁹S. Nowy, B. C. Krummacker, J. Frischeisen, N. A. Reinke, and W. Brütting, *J. Appl. Phys.* **104**, 123109 (2008).
- ¹⁰A. Drezet, F. Przybilla, E. Laux, O. Mahboub, C. Genet, T. W. Ebbesen, J. S. Bouillard, A. V. Zayats, I. S. Spevak, A. V. Kats, A. Yu Nikitin, and L. Martín-Moreno, *Appl. Phys. Lett.* **95**, 021101 (2009).
- ¹¹T. Onishi, T. Tanigawa, T. Ueda, and D. Ueda, *IEEE J. Quantum Electron.* **43**, 1123 (2007).
- ¹²P. B. Johnson and R. W. Christy, *Phys. Rev. B* **6**, 4370 (1972).
- ¹³A. Vial, A. S. Grimault, D. Macias, D. Barchiesi, and M. L. de la Chapelle, *Phys. Rev. B* **71**, 085416 (2005).
- ¹⁴S. G. Rodrigo, F. J. Garcia-Vidal, and L. Martín-Moreno, *Phys. Rev. B* **77**, 075401 (2008).
- ¹⁵E. D. Palik, *Handbook of Optical Constants of Solids* (Academic, New York, 1985).
- ¹⁶A. V. Zayats, I. I. Smolyaninov, and A. A. Maradudin, *Phys. Rep.* **408**, 131 (2005).
- ¹⁷A. Krishnan, T. Thio, T. J. Kim, H. J. Lezec, T. W. Ebbesen, P. A. Wolff, J. Pendry, L. Martín-Moreno, and F. J. Garcia-Vidal, *Opt. Commun.* **200**, 1 (2001).